

The Prediction and Measurement of the Optical Properties of Complex Surfaces

James Jafolla
Surface Optics Corporation
San Diego, CA 92127
www.surfaceoptics.com

Abstract

Determining the optical properties of complex surfaces for signature analysis can be problematic. Materials with surface structures, e.g. crinkled or patterned foil appliques, or striated or ribbed surfaces will produce a non-isotropic BRDF, which can be difficult to measure and represent in signature models. This paper will describe an analytical approach to predicting the optical properties of these surfaces. The calculations use a ray tracing algorithm and faceted model of the surface structure, materials and bulk optical properties. A comparison to measurements from the SOC 210 Bidirectional Reflectometer is presented. Also, the challenges of potential parameterized approaches for inclusion in signature models are discussed.

1.0 Introduction

A physically reasonable representation of the Bidirectional Reflectance Distribution Function (BRDF) is an important aspect for realistic CGI rendering applications and quantitative signature analysis. Some approaches for representing the BRDF are based on the assumption of homogeneous and isotropic surfaces (1,2). Some representations take into account the anisotropic nature of light scattering from surfaces and which account for surface structures and textures (3,4,5). These anisotropic BRDF models typically represent the surface features in a statistical fashion, often by fitting parameterized functions to BRDF measurements (5) or an analytic model base on a statistical micro-facet distribution function (3). Other models represent using phenomenological formulations for surface (including statistical roughness) and volume scattering contributions to the BRDF (6,7).

The approach described in this paper performs a direct calculation of the BRDF from complex surfaces by ray tracing light interactions on 3D facet model and a parameterized BRDF model of the facet optical properties.

2.0 Multiple Reflection BRDF Formulation

For a flat, homogeneous surface, the BRDF is defined as,

$$N_r(\theta_r, \phi_r) = H_o(\theta_o, \phi_o) \rho(\theta_o, \phi_o; \theta_r, \phi_r),$$

where $N_r(q_r, f_r)$ is the reflected radiance ($w/cm^2/sr$), $H_o(q_o, f_o)$ is the incident irradiance (w/cm^2), and $r(q_o, f_o; q_r, f_r)$ is the BRDF ($1/sr$). Or,

$$\rho(\theta_o, \phi_o; \theta_r, \phi_r) = \frac{\text{Reflected Radiance}}{\text{Incident Irradiance}} = \frac{N_r(\theta_r, \phi_r)}{H_o(\theta_o, \phi_o)}$$

Similarly, for the situation where the surface is directly illuminated by an external source and indirectly illumination by secondary reflections from within the surface, the BRDF is defined by the

ratio of the reflected radiance to the incident irradiance. For this case, the incident power (watts) on the surface due to direct and indirect illumination from surface, i , is given by,

$$\text{Illum} = H_o(\theta_o, \phi_o) A_d^k + \sum_i H_o(\theta_o, \phi_o) \rho_i(\theta_o, \phi_o; \theta_x, \phi_x) \Omega_x^i A_i^k$$

where, $\Omega_x^i = \cos \theta_x A_i^i / r_{ik}^2$ is the projected solid angle of facet, i , viewed by facet, k , and A_d^k is the directly illuminated area of facet, k , and A_i^k is the area indirectly illuminated. The angles (q_x, f_x) provide the direction of the light reflected from facet, i , to facet, k , and $r_i(q_o, f_o; q_x, f_x)$ is the BRDF of facet, i , that provides the illumination on facet, k , and the summation is over all facets which can illuminate facet, i . Figure 1 shows the geometry for this interaction.

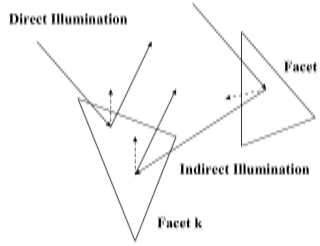


Figure 1. The geometry of direct and indirect illumination between facets.

The reflected intensity (watts/steradian) can also be written in terms of both the directly and indirectly incident rays,

$$\begin{aligned} \text{Ref} = & H_o(\theta_o, \phi_o) \rho^i(\theta_o, \phi_o; \theta_r, \phi_r) A_d^k \\ & + \sum_i H_o(\theta_o, \phi_o) \rho^i(\theta_o, \phi_o; \theta_x, \phi_x) \rho^k(\theta_x, \phi_x; \theta_r, \phi_r) \Omega_x^i A_i^k \end{aligned}$$

which is given in terms of the incident power and the BRDF of facet, k . The effective BRDF for facet, k , including direct and indirect illumination is then given by,

$$\rho_k^{\text{eff}}(\theta_o, \phi_o; \theta_r, \phi_r) = \text{Ref} / \text{Illum}$$

or, dividing by the incident irradiance,

$$\rho_k^{\text{eff}} = \frac{\rho_k(\theta_o, \phi_o; \theta_r, \phi_r) A_d^k + \sum_i \rho_i(\theta_o, \phi_o; \theta_x, \phi_x) \rho_k(\theta_x, \phi_x; \theta_r, \phi_r) \Omega_x^i A_i^k}{A_d^k + \sum_i \rho_i(\theta_o, \phi_o; \theta_x, \phi_x) \Omega_x^i A_i^k}$$

Finally, summing the effective BRDF for each facet, k , weighted by the unblocked, projected area of facet k , A_v^k , from the viewing direction (q_r, f_r) ,

$$\rho_{Surface}^{eff}(\theta_o, \phi_o; \theta_r, \phi_r) = \frac{\sum_k \rho_k^{eff}(\theta_o, \phi_o; \theta_r, \phi_r) A_v^k}{\sum_k A_v^k}$$

gives the effective BRDF for the surface.

The key to evaluating the equation above is an accurate ray-tracing calculation that includes the effects of internal blockages and reflections within the structure of the surface. This is performed for each facet defined in the surface, and computes the unblocked area of the facet that receives both direct illumination and indirect illumination from all other facets.

The calculation starts with a loop that considers each facet in the model. First, blockages of facet i , by all other facets, k , are calculated. This is performed twice, once for the incident direction and once for the viewed direction to calculate the direct illumination/viewed contribution to the BRDF.

The collection of unblocked pieces of facet i that receive illumination are now considered as sources of indirect illumination on all other facets in the model. Another loop over all facets, k , is performed to calculate which facets receive indirect illumination due to specular reflection from the piece of the i -th facet. The collection of facets receiving reflection are then analyzed with yet another loop over all facets in order to compute any internal blockages between the illuminating facet and the facet receiving the indirect illumination.

3.0 Surface Definition

While the BRDF of arbitrary complex surfaces can be computed in this way, it is of interest to study surfaces with repeating, regular surface features. Siegel and Howell (8) studied surface structures with parallel, truncated grooves as a technique for modifying the directional emissivity of a surface for thermal radiation heat transfer.

This study focused on four sided triangular pyramids with a square base, shown in Figure 2. The figure also shows the facet model definition of the surface. One advantage of this modeling approach is that the optical properties of each facet can be specified from the measured and/or modeled BRDF of the homogeneous and isotropic optical properties of the facet material or surface coating, similar to the surface features described in Siegel and Howell study.

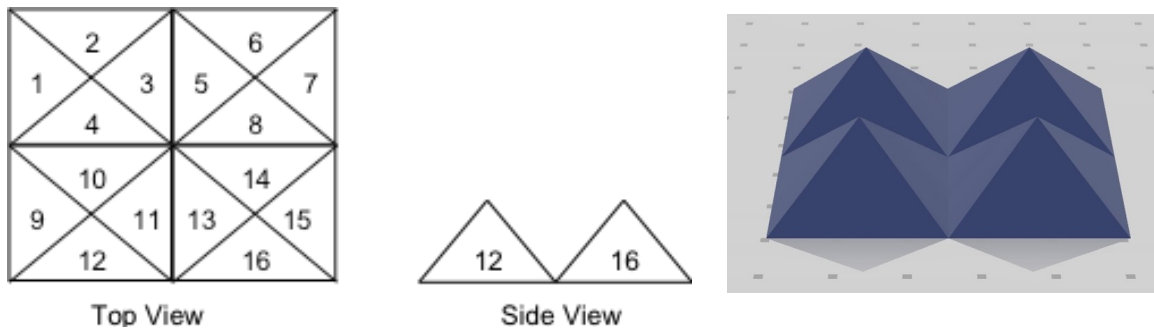


Figure 2. Model representation of a four-sided triangular pyramid.

Also, given the nature of a regular, repeating surface features, the analysis only needs to consider a small number of facets that capture the possible interactions between the surface features, which significantly reduces the computation time. This was verified by comparison of the results of simulations using 4, 12, and 48 pyramid surface models.

This surface was manufactured by machining a flat aluminum panel with parallel V-grooves, then rotating the sample by 90 degrees and repeating the process. This resulted in the regular array of four sided pyramids shown in Figure 3.

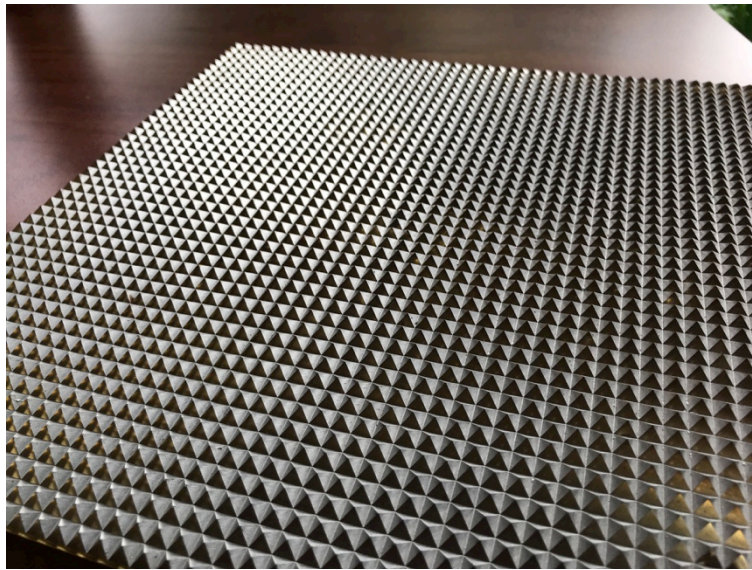


Figure 3. Manufactured sample of pyramidal surface structure.

4.0 BRDF Measurements and Parameterization

The BRDF measurements were performed using the SOC 210 Bidirectional Reflectometer shown in Figure 4. This is a goniometric instrument which measures and maps the BRDF over the upper hemisphere by scanning from 0 to 85 degrees in incident and reflected zenith angle, theta, and 0 to 350 degrees in incident and reflected azimuthal angle, phi at angular resolutions of up to 0.1 degree. The measurements are made with sources, discrete filters and detectors at wavelengths from 0.35 to 14 microns.

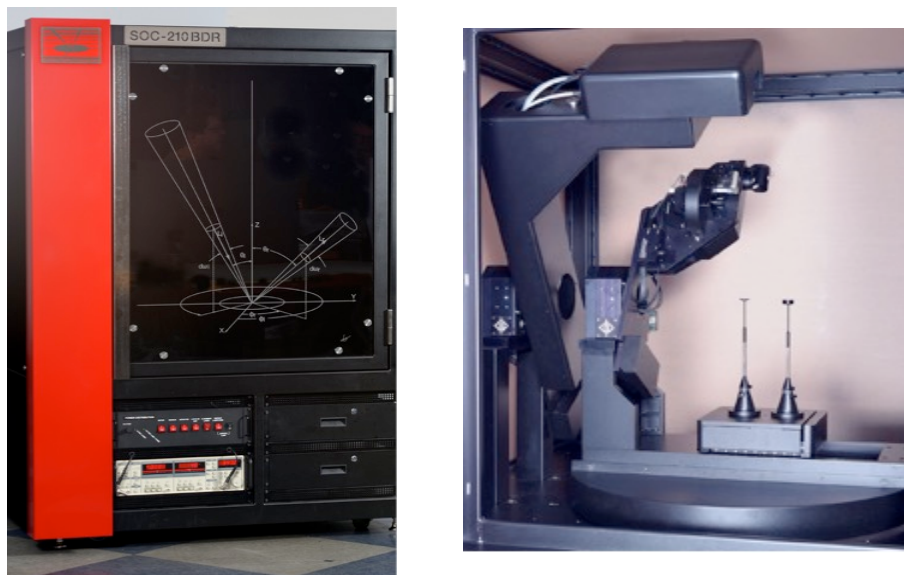


Figure 4. SOC 210 Bidirectional Reflectometer .

The geometry of the BRDF measurements is shown in Figure 5

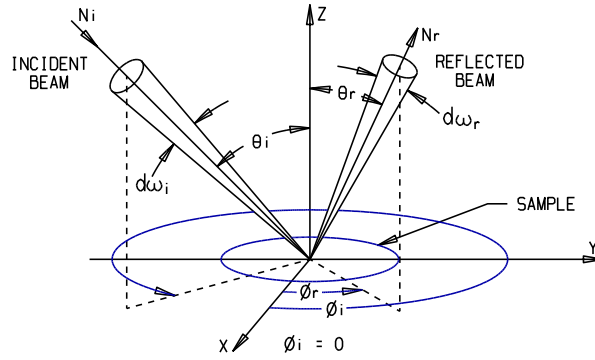


Figure 5. BRDF Geometry.

The BRDF is defined as the ratio of the reflected radiance ($w\cdot m^{-2}\cdot sr^{-1}$) in a particular direction (θ_r, ϕ_r) to the incident irradiance ($w\cdot m^{-2}$) from direction (θ_i, ϕ_i) .

$$\rho'(\theta_i, \phi_i, \theta_r, \phi_r) = \frac{\delta N_r(\theta_r, \phi_r)}{N_i(\theta_i, \phi_i) \cos \theta_i \delta \omega_i}$$

The units of the BRDF are inverse solid-angle (sr^{-1}).

Figure 6 shows the measurements of a moderately diffuse, homogeneous grey paint sample for an incident angle of 40 degrees at 0.5 microns.

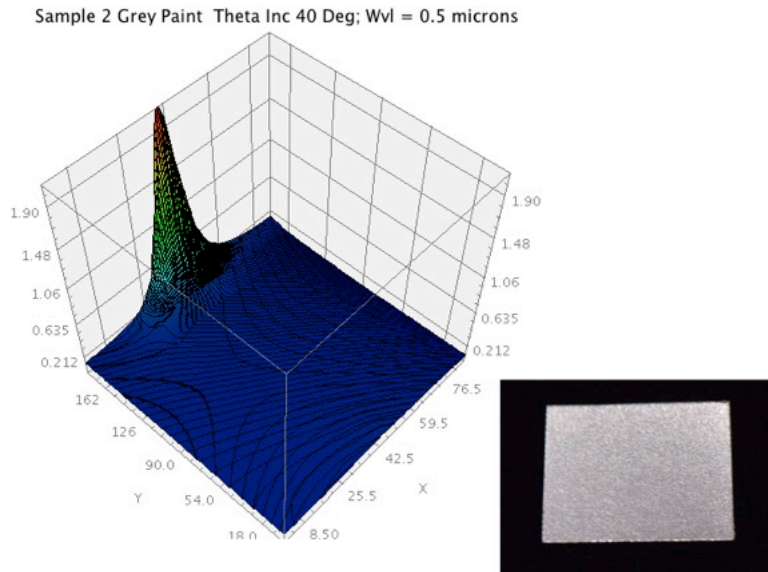


Figure 6. BRDF measurements of a moderately diffuse grey paint sample.

The Sandford-Robertson (SR) model (9) was chosen for this simulation because it does a good job representing moderately specular coatings and surfaces. It is based on the assumption that the angular properties of the BRDF vary slowly with wavelength and can be separated from the spectral characteristics.

$$\rho'(\hat{k}_i, \hat{k}_r; \lambda) = f_r(\hat{k}_i, \hat{k}_r) \rho(\lambda)$$

where \hat{k}_i is the unit vector to the light source, \hat{k}_r is the unit vector to the receiver, and $\rho(\lambda)$ is the total spectral hemispherical reflectance of the surface. It is further assumed the the angular dependence can be separated into a specular and diffuse component.

$$f_r(\hat{k}_i, \hat{k}_r) = f_D(\hat{k}_i, \hat{k}_r) + f_S(\hat{k}_i, \hat{k}_r)$$

The directional and spectral dependence of the emissivity is used to determine the diffuse scattering parameters, $\varepsilon(\lambda)$ and b , from spectral measurements

$$\begin{aligned} 1 - \rho(\theta, \lambda) &= \varepsilon(\theta, \lambda) \\ &= \varepsilon(\lambda) g(\theta) / G(b) \end{aligned}$$

where $\varepsilon(\lambda)$ is the total spectral emissivity. The grazing angle dependence is given by

$$g(\theta) = 1 / (1 + b^2 \tan^2 \theta)$$

and the normalization constant of the angular distribution is

$$G(b) = \frac{1}{1-b^2} \left[1 - \frac{b^2}{1-b^2} \log(1/b^2) \right]$$

The diffuse component of the BRDF is given by

$$f_D(\hat{k}_i, \hat{k}_r) = \frac{1}{\pi} g(\theta_r) \rho_D(\lambda) g(\theta_i) / G^2(b)$$

The specular component of the BRDF lobe is assumed to be a circular ellipsoid centered on the specular angle with eccentricity e , defined by

$$f_S(\hat{k}_i, \hat{k}_r) = \frac{1}{4\pi} \rho_S(\theta_i, \lambda) \frac{h(\alpha)}{H(\theta_i) \cos \theta_r}$$

where

$$h(\alpha) = \frac{1}{(e^2 \cos^2 \alpha + \sin^2 \alpha)^2}$$

with α being the angle between the glint vector and the surface normal

$$\begin{aligned} \hat{g} &= (\hat{k}_r - \hat{k}_i) / \sqrt{2(1 - \hat{k}_i \cdot \hat{k}_r)} \\ \cos \alpha &= \hat{g} \cdot \hat{n} \end{aligned}$$

and the normalization factor being

$$H(\theta_i) = \frac{1}{2e^2} [(1 - e^2) \cos \theta + \frac{2e^2 + (1 - e^2)^2 \cos^2 \theta}{(1 - e^2)^2 \cos^2 \theta + 4e^2}]$$

Thus, the four SR model parameters are:

$$\begin{aligned}\rho_D(\lambda) &= \text{diffuse spectral reflectance} \\ \varepsilon(\lambda) &= \text{spectral emissivity} \\ b &= \text{grazing angle reflectivity} \\ e &= \text{width of specular lobe}\end{aligned}$$

with an additional constraint for defining the energy in the specular lobe

$$\rho_S(\lambda) = G(b) - \rho_D(\lambda) - \varepsilon(\lambda)$$

The SR model fitting procedure involves fitting the $\varepsilon(\lambda)$ and b parameters to the spectral Directional Hemispherical Reflectance (DHR) from a separate measurement hemispherical measurements or by integrating the full angular mapping BRDF data set over all reflecting angles in the hemisphere. The b parameter is obtained by averaging the ratio of the near normal measurement to the measurements from 50 to 80 degrees. The $\rho_D(\lambda)$ and e parameters are obtained by iteratively adjusting the energy in the specular lobe and the shape so that a reasonable fit is achieved for each of the theta incident angles (e.g., 20, 40 and 60 degrees). The result of this fitting technique is shown in Figure 7 for the grey paint sample measurements shown in Figure 6..

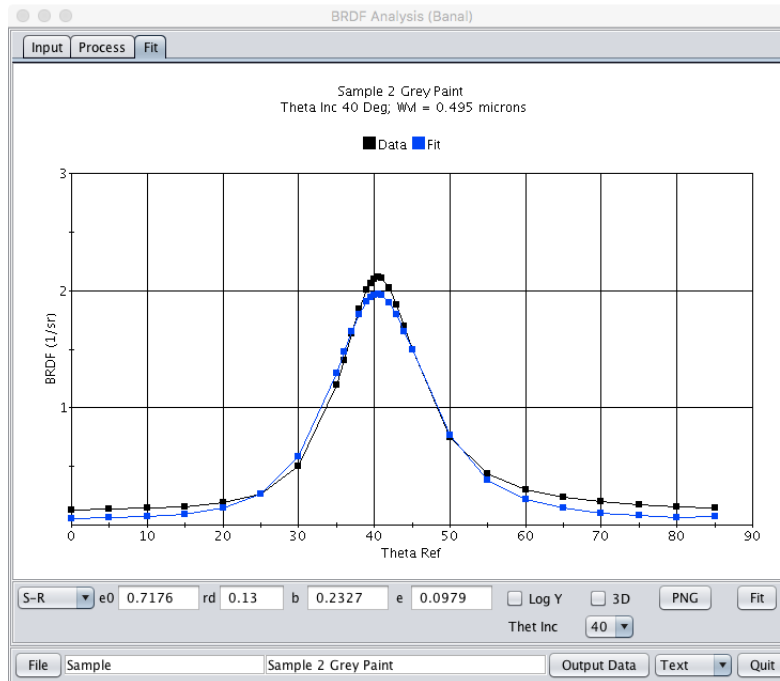


Figure 7. Comparison of Sandford-Robertson model fit to BRDF measurements of the grey paint sample.

One advantage of using a parameterized BRDF representation at the facet level in the simulation is that the facet optical properties can be quickly tuned to represent a variety of surface conditions. An example of this is shown in Figure 8. The optical properties are associated with individual facets and can represent non-homogeneous surface structures.

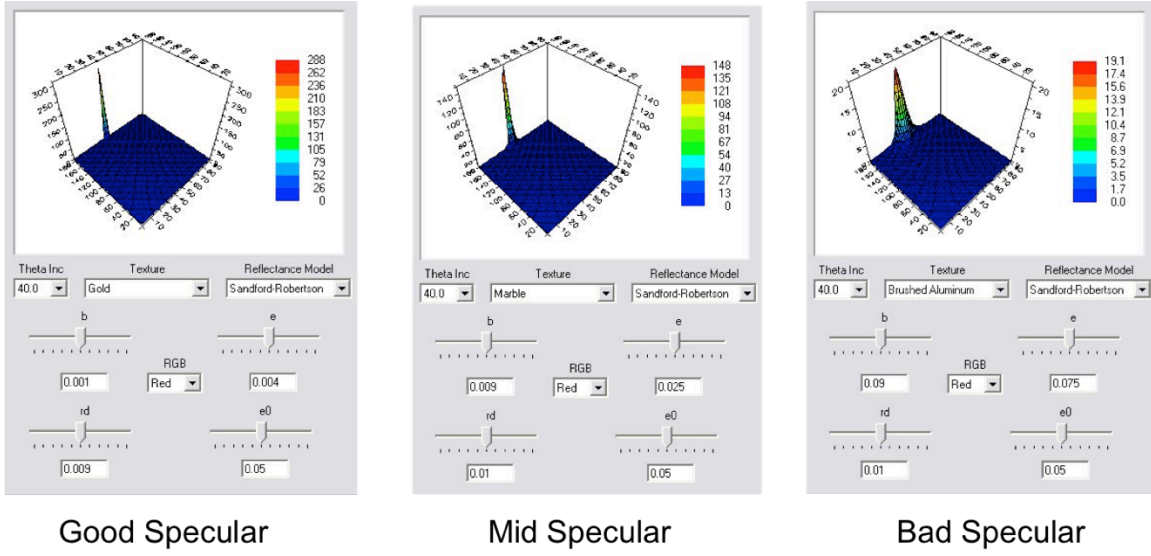


Figure 8. Sandford-Robertson parameterization of specular surfaces.

5.0 Model-Measurement Comparison and Implications For Signature Analysis

The results of the model calculations compared to the BRDF measurements are shown in Figure 9. Light was incident on the surface at 40 degrees from zenith, parallel to the grooves. Both the model and measurements show four distinct scattering lobes: a forward scattering (specular) lobe (theta 40, phi 180), two side scattering lobes (theta 50, phi 90 and theta 90, phi 135) and a broad backscattering feature (centered around theta 50, phi 0).

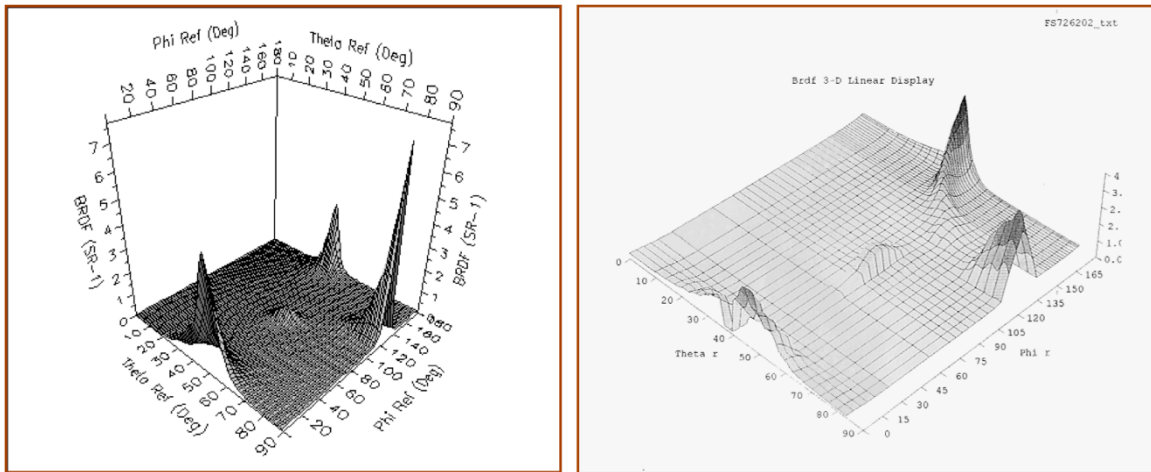


Figure 9. Comparison between predicted BRDF (left) and measurement for pyramid surface for a 40-degree incident angle.

All of the lobes agree well in position and magnitude given the instrumentation limitations. The measurement of the backscattered lobe shows the lack of data in the exact retro direction due to instrument blockages. The magnitude of the side-scattered lobe (phi 135) is consistent with the model at the limit of the instrument travel (85 degrees).

The forward scattering lobe in the measurements is also seen to have a skewed tail in theta-phi. This is consistent with BRDF features associated with micro grooves in the surface finish, probably from machine tooling marks. For this reason the Sandford-Robertson parameters used in this model were chosen to represent a “bad specular” BRDF (Figure 8). Interestingly, the calculations using the “good specular” finish resolved the broad backscattered feature into two lobes, one at exact retro (theta 40, phi 0) and one at theta 50 degrees.

Another model calculation was performed for a simple ridged surface shown in Figure 10. These calculations were performed at high resolution in all four angles, and for variations of surface finish. The results are best viewed as an animation as a function of the incident azimuth (phi) and zenith (theta) angles. Figure 11 shows a small subset of these results for the “bad specular” finish.

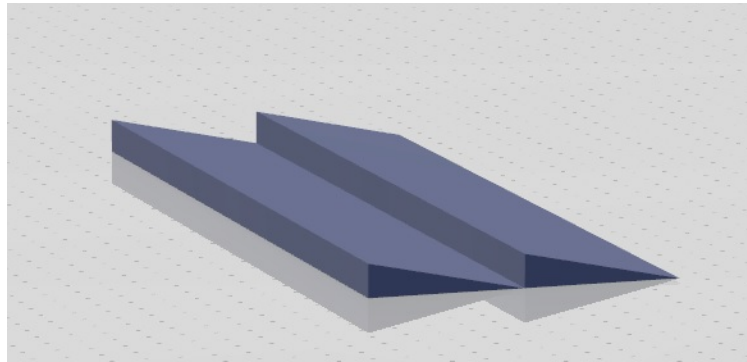


Figure 10. Grooved surface model.

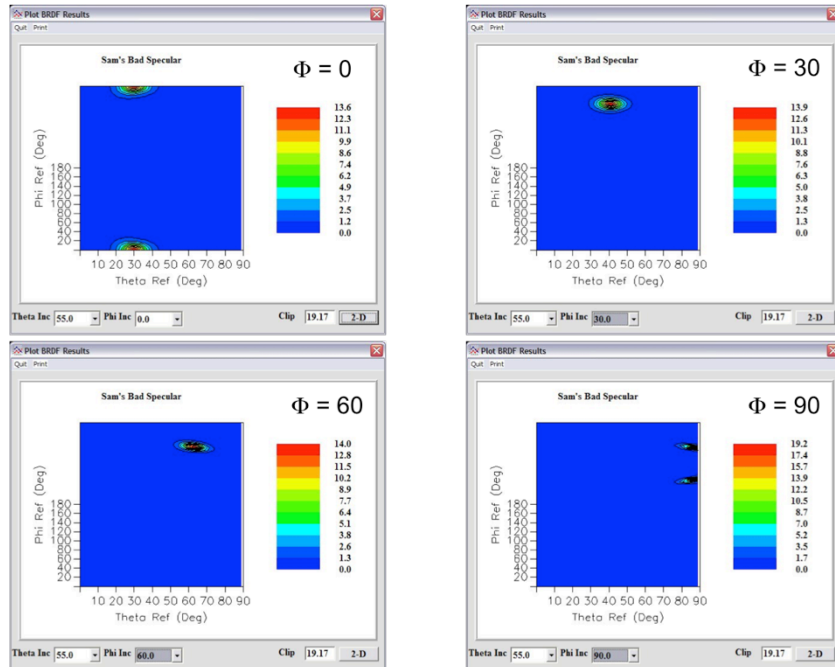


Figure 11. BRDF of grooved surface at incident theta 55 deg as a function of reflected phi.

One of the key insights obtained from this analysis is the understanding of the complexity and variability of light scattering from complex structured surfaces. Multiple reflections between macro-scale surface features produce multiple scattering lobes that can travel in angle, bifurcate and/or

combine together into a single scattering lobe. This has implications for accurate signature calculations of targets with surface treatments of this type. The empirical or parameterized BRDF models (10,11) typically used in signature calculations are not capable of capturing this complex phenomenology. At the same time, phenomenological models, such as the one described here, require significant computational resources and are not appropriate for the rapid BRDF evaluations required for signature calculations. Hilgers (10) has proposed an approach that fits multiple Gaussian lobes for each angle combination and introduces a tracking function to capture the movement of these lobes in angle space. More work is needed in this area to accurately capture these effects in signature calculations.

6.0 Conclusions

This study has described a phenomenology based approach to predicting the optical properties (BRDF) of non-homogeneous, complex surfaces using ray tracing and homogeneous surface BRDF models. The results have been validated by measurements of a manufactured material with regular, repeating surface features. These types of surfaces can be the result of design for thermal engineering applications or simply fabric like appliques.

The ability to capture this phenomenology in parameterized models for rapid signature calculations or CGI is currently somewhat problematic, and more work is needed.

References

1. B. Phong. "Illumination for computer generated pictures," *Commun. ACM* 18, 6 (June), 311–317, 1975.
2. J. Blinn. "Models of light reflection for computer synthesized pictures," In *Proceedings of SIGGRAPH 77*, 192–198, 1977.
3. M. Kurt, L. Szirmay-Kalos, and J. Krivanek. "An anisotropic BRDF model for fitting and Monte Carlo rendering," in *ACM SIGGRAPH Computer Graphics*, vol. 44, no. 1, 2010.
4. M. Ashikmin and P. Shirley. "An anisotropic Phong light reflection model," Technical Report UUCS-00-014, Computer Science Department, University of Utah, June 2000.
5. G Ward. "Measuring and modeling anisotropic reflection," *Computer Graphics*, 26(4):265–272, July 1992. ACM Siggraph '92 Conference Proceedings.
6. R. Cook and K. Torrance. "A reflectance model for computer graphics," In *Proceedings of SIGGRAPH 81*, 307– 316, 1981.
7. J. Jafolla, J. Stokes and R. Sullivan, "Phenomenological BRDF modeling for engineering applications," SPIE Vol. 3141, 1997
8. R. Siegel and J. Howell. "Thermal Radiation Heat Transfer," McGraw-Hill, pp 155-158, 1972
9. B. Sandford and D. Robertson. "Infrared reflectance properties of aircraft paints," IRIS Targets, Backgrounds and Discrimination, 1985.
10. J. Jafolla, D. Thomas and J Hilgers, "A comparison of BRDF representations and their effect on signatures," ADM201041, IRIS CONFERENCE PROCEEDINGS, 1998.
11. J. Jafolla and W. Reynolds, "Bidirectional reflectance measurements for high resolution signature modeling," SPIE Vol. 5431-22, 2004.